

Research on Improved Droop Control Strategy Based on Virtual Impedance

X M Liu¹, B C Lu², Z P Ren³ and R X Zhang⁴

¹ Liaoning University of Technology, Liaoning Province, China

² Liaoning University of Technology, Liaoning Province, China

³ Liaoning University of Technology, Liaoning Province, China

⁴ Liaoning University of Technology, Liaoning Province, China

E-mail: 2284777389@qq.com

Abstract. Due to the property of line impedance and other factors in micro-grid, power supplied by distributed generation units could not be shared accurately based on their traditional droop coefficient. To improve the power sharing accuracy of distributed generation units, improved droop control of power sharing strategy which was based on virtual impedance is proposed in this paper. Simulations results show that improved droop controller can achieve good load active and reactive power sharing.

1. Introduction

In recent years, distributed generation (DG) technology has been widely studied by scholars both at home and abroad. In order to cope with the flexible nature of DG and solve the problem of its reliable access, micro-grid is proposed as an effective solution [1]. A micro-grid can operate in parallel to grid or in island. The control technology of micro-grid is a key part of the operation of the micro-grid. Mature control technologies can improve the flexibility of micro-grid operation and improve power quality [2]. Droop control adjusts amplitude of the output voltage and frequency according to DG's output. The system distributes load according to droop coefficient. However, traditional droop control is generally considered to be used only when it is satisfied $X \gg R$. Traditional droop control of the low-voltage micro-grid running in island will cause frequency and voltage to deviate from the rated values. Power supplied by DG units could not be shared accurately based on their traditional droop coefficient [3]. In order to solve this problem, [4] proposed a whole-cycle adaptive adjustment method, so that the system could obtain high dynamic performance under different loads. [5] considered the linear impedance effect, and ignored linear resistance according to the linear relationship between the system output reactive power and line voltage drop. [6] proposed a control strategy for automatically adjusting the droop coefficient.

Based on the analysis of the droop characteristic, this paper analyses the reasons for the deviation of reactive power distribution. In order to reduce the error of power distribution, virtual impedance control loop is added to the traditional droop control so that DG in micro-grid can complete the decoupling control of power. Simulation result shows that the proposed scheme can effectively improve the power distribution relationship between DG units.

2. Analysis of droop characteristic

In the analysis of power flow for micro-grid, equivalent circuit of its power transmission which is shown in figure 1.



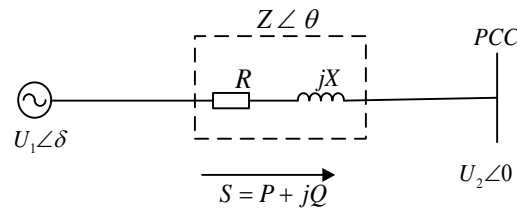


Figure 1. Power transmission equivalent model.

P and Q output from inverter are respectively shown in equations (2.1) and (2.2).

$$P = \left(\frac{U_1 U_2}{Z} \cos \delta - \frac{U_2^2}{Z} \right) \cos \theta + \frac{U_1 U_2}{Z} \sin \delta \sin \theta \quad (2.1)$$

$$Q = \left(\frac{U_1 U_2}{Z} \cos \delta - \frac{U_2^2}{Z} \right) \sin \theta - \frac{U_1 U_2}{Z} \sin \delta \cos \theta \quad (2.2)$$

Where, P and Q output by the inverter supply are related to the voltage amplitude, phase angle of inverter output and line impedance. There is a serious coupling.

(1) The impedance of the transmission line used by the high voltage micro-grid is much greater than resistance ($X \gg R$), so the effect of R can be ignored. Equations (2.1) and (2.2) can be written as:

$$P = \frac{U_1 U_2 \sin \delta}{X} \quad (2.3)$$

$$Q = \frac{U_1 (U_1 - U_2)}{X} \quad (2.4)$$

Since phase angle is small, P can be adjusted by the phase angle. Q can be adjusted by voltage amplitude. This method is the traditional droop control ($P - f / Q - V$). Droop control equations are shown in (2.5) and (2.6):

$$f - f_N = k_p (P_N - P) \quad (2.5)$$

$$U - U_N = k_q (Q_N - Q) \quad (2.6)$$

(2) The low voltage micro-grid exhibits pure resistance. Equations (2.1) and (2.2) can be written as:

$$P = \frac{U_1 (U_1 - U_2)}{R} \quad (2.7)$$

$$Q = \frac{U_1 U_2 \sin \delta}{R} \quad (2.8)$$

Droop control equations are shown in (2.9) and (2.10):

$$f - f_N = k_q (Q_N - Q) \quad (2.9)$$

$$U - U_N = k_p (P_N - P) \quad (2.10)$$

Figure 2 uses the same capacity inverter with the same droop coefficient as an example to analyse the causes of reactive power error. (E_1, Q_1) and (E_2, Q_2) are the actual operating points for two inverters operating in parallel. It can be seen that the output reactive power is unbalanced due to the different line impedances [7].

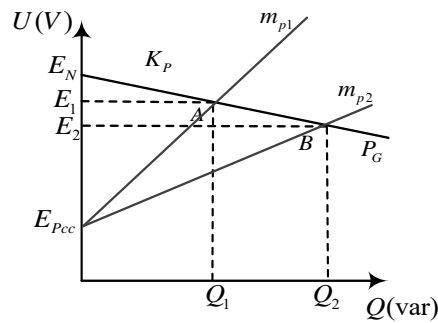


Figure 2. Traditional Q-V droop control.

From equations (2.4) and (2.6), it can be approximated as follows:

$$\Delta Q_{err} = \frac{Q_1 - Q_2}{Q_1} \approx \frac{R_2 - R_1}{R_2 + K_q E_{PCC}} \tag{2.11}$$

From equation (2.11), the distribution error is related to the line impedance, droop coefficient and inverter output voltage.

In summary, the transmission impedance components of lines are diverse and the use of two droop control is cumbersome. In order to solve this problem, this paper introduces a virtual impedance to cover the previous impedance, that is, the virtual impedance method.

3.Improved droop control strategy based on virtual impedance

3.1Power decoupling analysis of virtual impedance is introduced

The virtual impedance method firstly obtains the inductor current, I_0 , at the output side of the inverter through sampling. I_0 multiplied by Z_v to form a feedback loop. U_{ref} is obtained according to the traditional droop control. U_{ref} minus the voltage drop from the virtual impedance is the U_{ref}^* . Then passes the voltage outer loop PI control link and current inner ring P control link, finally obtain SPWM modulation signal control the inverter. Express it as equation (3.1):

$$U_{ref}^*(s) = U_{ref}(s) - Z_v(s)I_0(s) \tag{3.1}$$

Figure 3 shows an equivalent system diagram with virtual impedance added. The impedance between the DG and the bus in low voltage micro-grid $Z_L = R + jX$ is resistive without adding the virtual impedance. First is to remove the DG and add a virtual generator, VG, which is still connected to the N point through the virtual impedance $Z_v = R_v + jX_v$. When $|X_v| \gg |Z_L|$, the sum of Z_v and Z_L is perceptual. Droop control is applied to VG, so that P_0 and Q_0 can be decoupled [8].

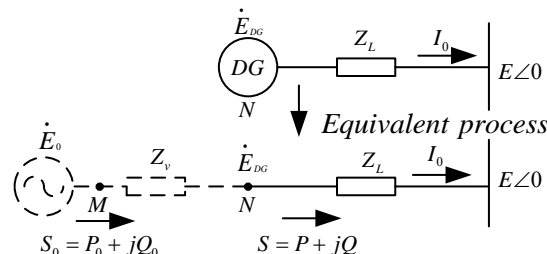


Figure 3. Equivalent system diagram after adding virtual impedance.

(1)Active power decoupling

The virtual impedance used here considers the inductance, since it does not lose active power on it. Therefore $P_0 = P$, and the decoupling control of M active power can be accomplished by changing the power angle, δ , of the virtual generator.

(2) Reactive power decoupling

Line impedance $Z_L = R + jX$, satisfy $\sin \theta = \frac{X}{Z}$ and $\cos \theta = \frac{R}{Z}$. Substitute it into equation (3.2):

$$Q = \frac{U_2}{|Z|} [(U_1 \cos \delta - V) \sin \theta - U_1 \sin \delta \cos \theta] \quad (3.2)$$

After finishing:
$$Q = \frac{U_2}{R^2 + X^2} [(U_1 \cos \delta - U_2)X - U_1 R \sin \delta] \quad (3.3)$$

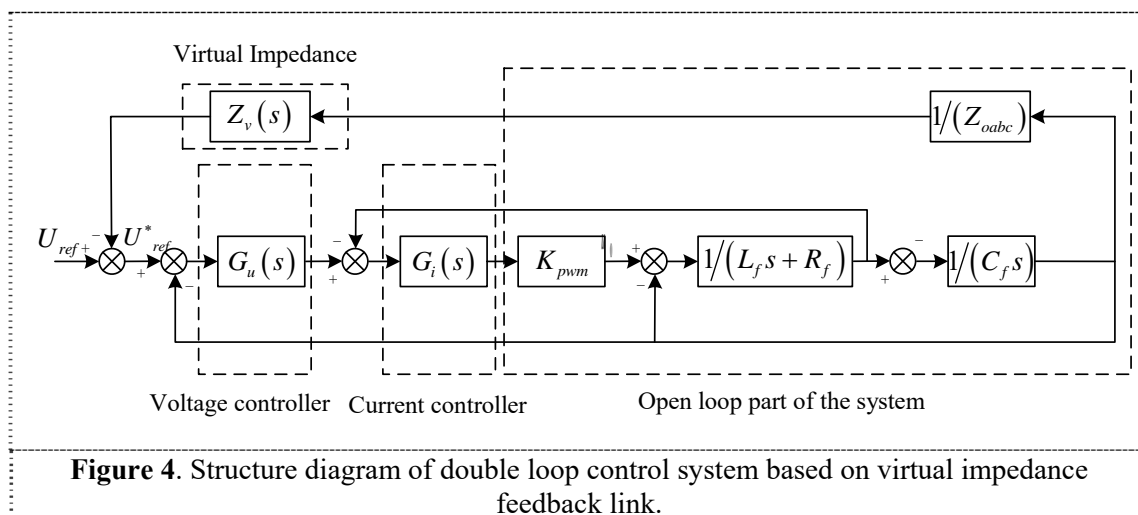
At point M, $Z_M = R + j(X + X_v)$. According to equation (3.3):

$$Q_N \approx \frac{U_2 [(E_0 - U_2)(X_v + X) - X_v (E_0 - U_2)^2]}{R^2 + (X + X_v)^2} = \frac{(E_0 - U_2)(U_2 X - E_0 X_v + 2U_2 X_v)}{R^2 + (X + X_v)^2} \quad (3.4)$$

According to equation (3.4), Q decoupling control of N point can be realized by changing E_0 .

3.2 Improved droop control strategy by introducing virtual impedance

Figure 4 shows the structure of a dual-loop control system based on a virtual impedance feedback loop. The essence of the virtual impedance introduced in figure 4 is to multiply the collected current signal by the virtual impedance value and introduce it into the voltage regulator, which helps to increase the stability of the system and reduce the influence of the circulation [5].



In order to make the system have good stability and dynamic response speed, voltage outer loop and current inner loop adopt PI control and P control respectively. $G_u(s)$ and $G_i(s)$ are shown as equations (3.5) and (3.6) respectively:

$$G_u(s) = K_{up} + K_{ui}/s \quad (3.5)$$

$$G_i(s) = K_{ip} \quad (3.6)$$

In the equations (3.5) and (3.6), K_{up} is proportional coefficient of the voltage outer loop PI controller.

K_{ui} is integral coefficient of the voltage outer loop PI controller. K_{ip} is proportional coefficient of the current inner loop P controller.

Different from traditional droop control, this article adds a control loop to the traditional droop control. After adding, the voltage reference can be expressed as equation (3.1). Substitute equation (3.1) into $U_0 = G_u(s)U_{ref}^* - Z_0(s)I_0(s)$. It can be expressed as equation (3.7):

$$U_0 = G(s)U_{ref} - [Z_0(s) + G(s)Z_v(s)]I_0 \quad (3.7)$$

$$G(s) = \frac{k_{ip}k_{up}k_{pwm}S + k_{ip}k_{ui}k_{pwm}}{LCS^3 + (k_{ip}k_{pwm} + r)CS^2 + (k_{ip}k_{up}k_{pwm} + 1)S + k_{ip}k_{ui}k_{pwm}} \quad (3.8)$$

$$Z_0(s) = \frac{(k_{ip}k_{up}k_{pwm}L_v + L)S^2 + (k_{ip}k_{ui}k_{pwm}L_v + k_{ip}k_{pwm} + r)S}{LCS^3 + (k_{ip}k_{pwm} + r)CS^2 + (k_{ip}k_{up}k_{pwm} + 1)S + k_{ip}k_{ui}k_{pwm}} \quad (3.9)$$

Where, $G(s)$ is the voltage gain transfer function. $Z_0(s)$ is the equivalent output impedance of the closed-loop system of the inverter.

After adding the new virtual impedance, the new equivalent output impedance is $Z_{ov}(s)$. The voltage proportional gain function is $G(s)$. R_v can be ignored. It can be expressed as equation (3.10):

$$Z_{ov}(s) = Z_0(s) + G(s)Z_v(s) \quad (3.10)$$

From equation (3.10), after introducing virtual impedance feedback link, the impedance characteristic of the inverter output can be flexibly changed, improving the droop characteristic [4].

4. Simulation analysis

In order to verify the improved droop control scheme proposed in this paper, the micro-grid system as shown in figure 5 is built in the Matlab/Simulink environment for simulation.

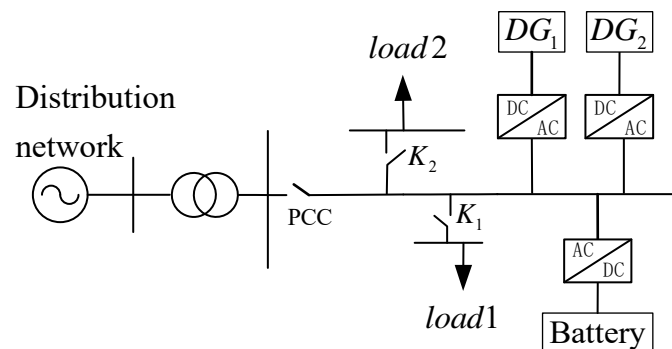


Figure 5. Micro-grid architecture.

Example 1 verifies the influence on the distribution of power before and after the virtual impedance is introduced under the condition that the droop coefficient is equal and the load changes. Example 2 verifies the influence of the distribution of power before and after the virtual impedance is introduced under the condition that the droop coefficient is not equal and the load changes. The simulation time is set to 10s. K_1 closed at 1s and disconnected at 7s. K_2 closed at 4s.

Example 1: When the droop coefficient of DG_1 and DG_2 is equal.

When no virtual impedance is added, the active power output from the two inverters which is shown in figure 6 and the reactive power in figure 7.

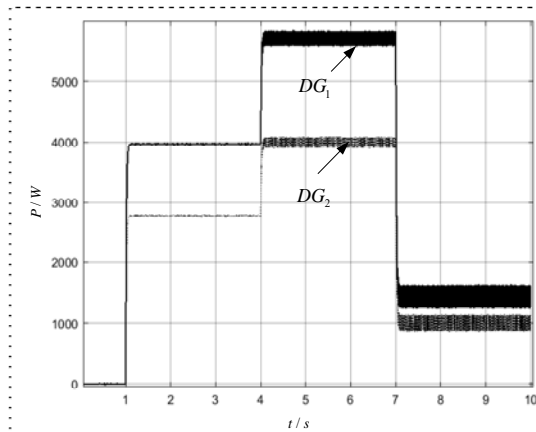


Figure 6. Active power of DG_1 and DG_2 without virtual impedance.

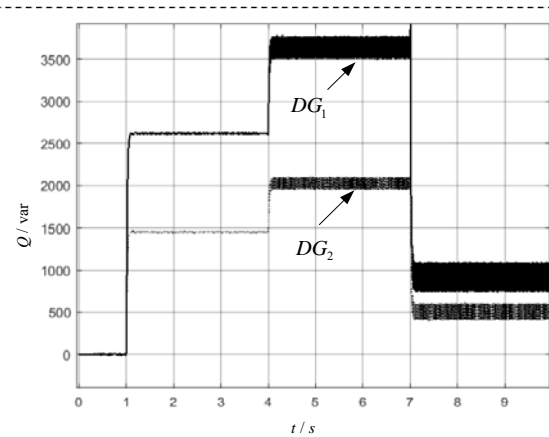


Figure 7. Reactive power of DG_1 and DG_2 without virtual impedance.

Due to the power coupling between active and reactive power, even if the droop coefficient is considered to be the same, the active and reactive power cannot be evenly distributed during the load switching process.

When virtual impedance is added, the active power output from the two inverters which is shown in figure 8 and the reactive power in figure 9.

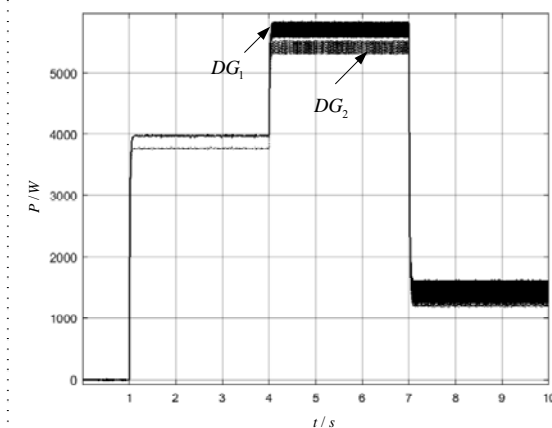


Figure 8. Active power of DG_1 and DG_2 with virtual impedance.

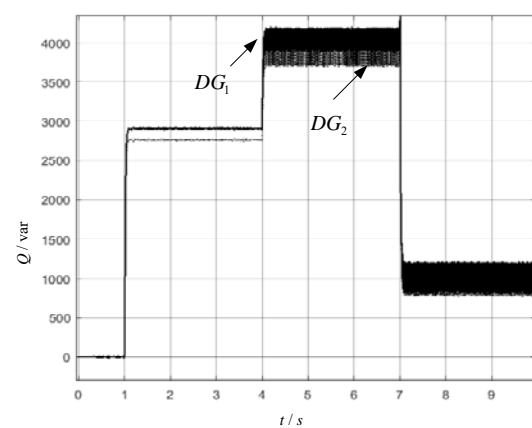


Figure 9. Reactive power of DG_1 and DG_2 with virtual impedance.

From Figure 8 and Figure 9, in the case of adding virtual impedance, the average distribution of active and reactive power is realized in the process of changing. The disturbance of the system is reduced, and the decoupling control of active and reactive power is realized.

Example 2: When droop coefficient of DG_1 and DG_2 is 1:2.

(1) When no virtual impedance is added, the active power output from the two inverters which is shown in figure 10 and the reactive power in figure 11.

Due to the existence of power coupling between active and reactive power, the active power and reactive power of the output cannot be allocated strictly in accordance with 2:1 in the switching load process.

(2) When virtual impedance is added, the active power output from the two inverters which is shown in figure 12 and the reactive power in figure 13.

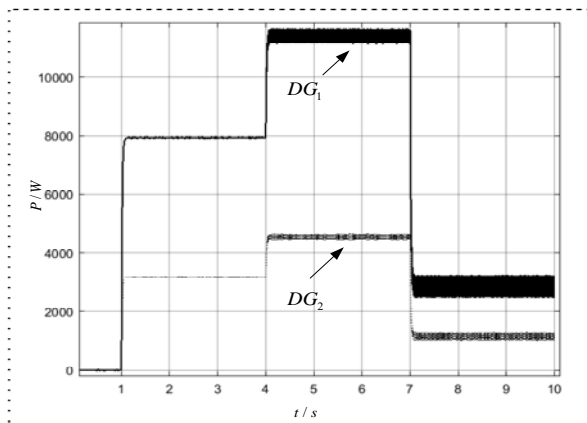


Figure 10. Active power of DG_1 and DG_2 without virtual impedance.

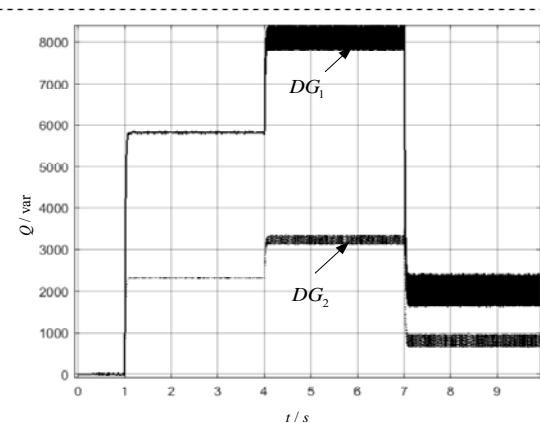


Figure 11. Reactive power of DG_1 and DG_2 without virtual impedance.

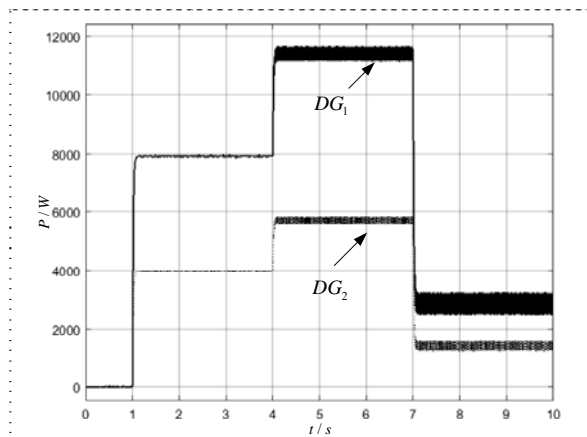


Figure 12. Active power of DG_1 and DG_2 with virtual impedance.

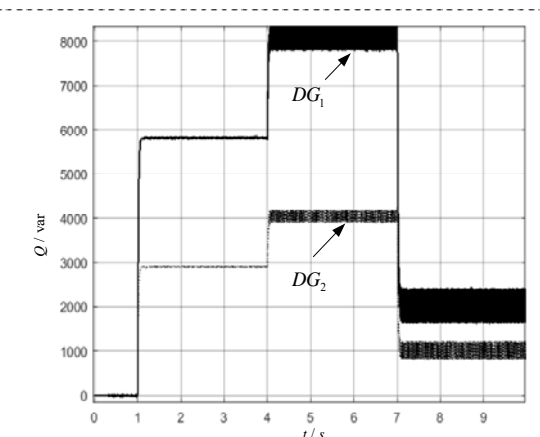


Figure 13. Reactive power of DG_1 and DG_2 with virtual impedance.

By adding a virtual impedance in the process of switching load, the active and reactive power output can basically be allocated according to the droop coefficient, which reduces the system disturbance and enables the decoupling control of active and reactive power.

5. Conclusion

Due to the influence of line impedance, the power of droop control unit running in parallel cannot be reasonably distributed. In this paper, the traditional P - f and Q - V droop control was improved. The virtual impedance control loop was added to traditional droop control, so that DG in micro-grid can complete the decoupling control of power. The improved droop control can effectively perfect the power distribution relationship between the DG units. The active and reactive power output can basically be allocated according to the droop coefficient.

Due to the time limit, there are still many deficiencies in this paper, which requires further research in the later stage, mainly including:

During the simulation, when the load power varies greatly, it is difficult to maintain the micro-grid's voltage and frequency at the rated value.

When the value of the virtual impedance is large, the inverter output voltage decreases.

6. References

- [1] Wu T, Liu Z and Liu J 2016 *IEEE Trans. Power Electron.* **31**(8) 5587-5603
- [2] Zhu S S, Wang F, Guo H, Wang Q F and Gao Y X 2018 *Proc. Chin. Soc. Electr. Eng.* **38**(01) 72-84 (in Chinese)

- [3] Wang C S, Li W, Wang Y F, Meng Z and Yang L 2017 *Proc. Chin. Soc. Electr. Eng.* **37(01)** 84-97 (in Chinese)
- [4] Zhu Y X, Fang Z, and Fang W 2015 *IEEE Trans. Power Electron.* **30(12)** 6706-19
- [5] Guo L, Feng Y B and Li X L 2016 *Proc. Chin. Soc. Electr. Eng.* **36(4)** 927-936 (in Chinese)
- [6] Mahmood H, Michaelson D and Jiang J 2015 *IEEE Trans. Power Electron.* **30(3)** 1605-17
- [7] Sun X F, Liu B J, Chen D, Wang B C and Wang D Y 2017 *Power Acta. Energi. Sin.* **38(02)** 309-316 (in Chinese)
- [8] Cheng Q M, Gao J, Cheng Y M, Zhang Y, Yu D Q and Tan F R 2018 *Power Sys. Techno.* **42(01)** 203-209 (in Chinese)

7.Acknowledgment

This work is supported by Education Committee Foundation of Liaoning province (JFL201715401).